Non-invasive ^{89}Zr-Transferrin PET Shows Improved Tumor Targeting Compared to ^{18}F-FDG PET in MYC-overexpressing Human Triple Negative Breast Cancer

Kelly E. Henry,[1] Thomas R. Dilling,[1] Dalya Abdel-Atti,[1] Kimberly J. Edwards,[1] Michael J. Evans,[2] Jason S. Lewis[1*]

[1]Memorial Sloan Kettering Cancer Center, Department of Radiology, 1275 York Avenue, New York, NY, 10065
[2]University of California San Francisco, Department of Radiology and Biomedical Imaging, 185 Berry Street, San Francisco, CA, 94107

SUPPLEMENTAL DATA

MATERIALS AND METHODS

Cell Lines and BRD4 Inhibitors. TNBC cell lines (MDA-MB-231, MDA-MB-157, and Hs578T) were obtained from the American Type Culture Collection (ATCC). All cells were grown according to the recommendations of ATCC under 37 °C with 5% CO_2 in a humidified atmosphere. All tissue culture manipulations were performed using sterile techniques. TNBC cells were treated with JQ1 (purchased from ApexBio) and OTX015 (purchased from Cayman Chemical) at 0.5-1 μM. All BRD4 inhibitors were confirmed to be >99% pure via in-house quality control assessment.

Cell Cycle Analysis. To confirm the antiproliferative effects of BRD4 inhibitors in TNBC cells and determine the point of cellular arrest, a flow cytometry assay using 5-ethynyl-2'-deoxyuridine (EdU) incorporation was performed. TNBC cells were seeded in 6-well plates (5×10^5) and incubated at 37 °C with 5% CO_2 in a humidified atmosphere overnight. Cells were incubated with fresh media, media with 0.5-1 μM drug (JQ1 or OTX015), or vehicle control (DMSO at matching concentrations) for 24 h. Post-drugging, EdU (10 μM) was added directly to the cells (without disruption) and incubated for 1 h at 37 °C. Cells were immediately harvested and washed twice with cold PBS and incubated with Fixable Live/Dead viability dye (488 nm excitable) which can withstand the fixing process required for this protocol. Cells were then

subjected to the Click It EdU System Protocol™ for staining with AlexaFluor647 (AF_{647}). The AF_{647} staining combined with 4',6-diamidino-2-phenylindole (DAPI, 3.6 μM) was used to resolve cell cycle phases in a given population into G_0/G_1, S, and G_2/M phase. Non-viable cells were gated out with the 488 nm excitable Fixable Live/Dead viability stain and data was analyzed by FlowJo software and plotted using GraphPad (PRISM).

Western blot. TNBC cells were plated in 100 mm culture dishes at 3×10^6 cells/dish. Cells were incubated with fresh media with vehicle (DMSO) or drug (0.5 μM of JQ1 and OTX015) and incubated for 24, 48, and 72 h. Cells were harvested and chemically lysed with RIPA buffer with protease inhibitor cocktail and phosphatase inhibitors (EMD Millipore, 1:100 dilution for each inhibitor). Cells were then subjected to mechanical lysis via sonication pulses at 4 °C (10 s on, 10 s off) for 10 min. Cell debris was then pelleted via centrifugation at 14000 rpm. Supernatant was analyzed for total protein content using a Lowry assay with a BSA standard curve. Lysates were prepared at 2 μg/mL total protein content with 4× SDS-PAGE loading dye, boiled for 5 min at 95 °C, and stored at -20 °C until use. Samples were loaded onto 7% tris-acetate gels and subjected to dry transfer via iBlot to nitrocellulose membranes. Ponceau red (0.5% w/v) was used to confirm protein transfer and membranes were blocked in 5% non-fat dry milk in TBS buffer with 0.1% tween for 1 h at room temperature. Blots were then incubated overnight with primary antibodies (anti-MYC: Cell Signaling, clone # D84C12, 500:1 dilution; anti-CD71: Cell Signaling, clone # D7S5Z, 1000:1 dilution; anti-β-actin, clone # AC-15, 20,000:1 dilution) at 4 °C in blocking solution. Blots were incubated with HRP-conjugated secondary antibodies (anti-mouse, abcam cat # ab6789, 7500:1 dilution; anti-rabbit, abcam cat # ab6721, 5000:1 dilution) for 1 h at RT. Detection of bands was performed with ECL signal substrate (GE Healthcare).

Quantitative real-time PCR. Quantitative RT-PCR was performed to quantify relative c-Myc and TfR (CD71) gene expression levels before and after treatment with BRD4 inhibitors, normalized to housekeeping gene expression (GAPDH). Cells were plated in 12-well plates at 3 × 10^5/mL, allowed to adhere overnight, and incubated with fresh media with vehicle (DMSO) or drug (0.5-1 μM JQ1 and OTX015). From the collected cell pellets, cells were lysed using QIAShredder and mRNA was extracted using a QIAGEN RNeasy isolation kit. Isolated mRNA was converted to cDNA using a 1 μg of mRNA product and an Applied Biosystem high capacity cDNA conversion reverse transcriptase kit with random primers. Aliquots of cDNA were quantified and prepared for triplicate reactions in a qRT-PCR plate using TaqMan Fast Advanced Master Mix and c-Myc (Assay # Hs00153408 and TfR (CD71) TaqMan polymerase gene assays (Assay # Hs00951083) Data was normalized with respective housekeeping genes (GAPDH, assay # Hs03929097) and no template controls were included as negative controls.

Flow Cytometry. Flow cytometry using a phycoerythrin (PE) labeled anti-CD71 (TfR) antibody (clone # CY1G4) to assess surface TfR protein levels pre- and post-drug treatment with BRD4 inhibitors in TNBC cells. Cells were plated in 6-well plates at 3 × 10^5/mL, allowed to adhere overnight, and incubated with fresh media with vehicle (DMSO) or drug (0.5-1 μM of JQ1 and OTX015) for 48 h. Post-incubation, cells were washed twice with PBS, trypsinized, and centrifuged to collect pellets. The cells were resuspended in Fc receptor blocking solution (Miltenyi Biotec) for 30 min to prepare for surface antigen staining (TfR), and analyzed via flow cytometry. DAPI was used as a viability marker for surface staining experiments. A PE-labeled IgG (clone # MOPC-173) was used as an isotype control to confirm specific binding to CD71 in TNBC cells. Data was analyzed by FlowJo software and plotted using GraphPad (PRISM).

Small interfering RNA (siRNA) transfection. TNBC cells were seeded in 12-well plates at 1× 10^5 cells/well in antibiotic-free medium and incubated overnight. Dharmafect siRNA (c-MYC, 50 nM) was administered to TNBC cells in antibiotic-free medium. Non-targeted siRNA pool was also administered at matching concentrations, along with untreated cells and GAPDH-targeted siRNA as controls. Quantitative RT-PCR was performed to quantify relative c-Myc and TfR (CD71) gene expression levels before and after treatment as described above. Protein analysis was performed via western blot using the same protocol as described above.

Internalization Assays with BRD4 Inhibitors. Holo-Tf (2 mg) was labeled with ^{131}I (74 Bq) using iodogen activation for 15 min in PBS. Purification was accomplished in a 30-kDa molecular weight cutoff Amicon filter column with 3× PBS (pH 7.4) washes. Tf labeling was assessed via instant thin-later chromatography (iTLC) with a mobile phase of 10% TFA to detect any ^{131}I not incorporated into the protein. Cells were plated at 3 × 10^5/mL, allowed to adhere, and incubated with fresh media with vehicle (DMSO) or drug (0.5 μM of JQ1 and OTX015) for 48 h. Radiochemical yield for each experiment was >95% and radiochemical purity was 99%. Cells were incubated with fresh media or media with ^{131}I-TF (0.037 MBq/well) for 1 h at 37°C. Media (with or without radiotracer) was removed, and the cells were washed twice with PBS, and trypsinized. Duplicate plates were used and treated the same for both protein quantification (for data normalization) and γ counting.

Preparation and Radiolabeling of ^{89}Zr-DFO-transferrin. Apo-transferrin was functionalized with p-isothiocyanatobenzyl-desferrioxamine (DFO-Bz-NCS; Macrocyclics, Inc.) and characterized to have one chelate per protein molecule via isotopic dilution assay (*1*). The DFO-modified protein was purified via a PD10 desalting column (GE Healthcare). The precursor was manufactured under Good Manufacturing Process and obtained from the Radiochemistry and

Molecular Imaging Probes Core at Memorial Sloan Kettering Cancer Center. ^{89}Zr was produced through proton beam bombardment of yttrium foil and isolated in high purity as ^{89}Zr-oxalate at Memorial Sloan Kettering Cancer Center according to a previously published procedure (1). ^{89}Zr-oxalate (37 Bq) was neutralized to pH 7.0–7.4 with 1 M Na_2CO_3. The DFO-Tf was added (100 μg) and the reaction was incubated at room temperature for 1 h. Subsequent purification was conducted using a PD10 desalting column with PBS. Purity and radiolabeling yields were quantified through iTLC with a 50 mM EDTA (pH 5) mobile phase.

Internalization Assays: Time Course. Tf was radiolabeled with ^{89}Zr as described above. TNBC cells were incubated with fresh media or media with ^{89}Zr-Tf (0.037 MBq/well) for 1.5 h at 37°C, with samples collected at multiple time points (15, 30, 45, 60, and 90 minutes). Media (with radiotracer) was removed at multiple time points, the cells were washed twice with PBS, rinsed with 100 mM acetic acid, 100 mM glycine, pH 3 to remove surface-bound tracer, and lysed with 1 M NaOH to collect internalized fraction. Duplicate plates were used and treated the same for both cell count (for data normalization) and γ counting.

Small Animal Models. All animal studies were conducted in accordance with the guidelines set by the Institutional Animal Care and Use Committee. Female athymic nude (NU/NU) mice (Charles River Laboratories, 6-8 weeks, 20-22 g) were inoculated with TNBC tumors. Cells were implanted orthotopically (5×10^6 cells) in the lower right mammary fat pad in 50 μL of 1:1 Matrigel (BD Biosciences) and grown to a tumor volume 150-200 mm^3 before use.

Patient-Derived Xenografts. TNBC patient-derived xenograft model (M24) were a kind gift from the Baselga Lab at Memorial Sloan Kettering Cancer Center and were inoculated subcutaneously on the flank in a suspension with Matrigel (1:1).

^{18}F-FDG Imaging. ^{18}F-FDG was obtained from the Nuclear Pharmacy at Memorial Sloan Kettering Cancer Center on the morning of injection (13-15 MBq/injection). ^{18}F-FDG was acquired from Zevacor and specific activity ranged from 0.74 GBq/mL-11.1 GBq/mL at the end of synthesis. Mice were fasted overnight and anesthetized with 1.5%-2% isoflurane (Baxter Healthcare) for 30 min prior to PET imaging. All mice were imaged at 1 h post-injection (p.i.).

In Vivo Imaging. Mice were anesthetized with 1.5%-2% isoflurane (Baxter Healthcare) in oxygen. PET imaging experiments were accomplished with a microPET Focus 120 (Concorde Microsystems). Mice were administered ^{89}Zr-labeled Tf (9-11 MBq, 100 μg) in 150-200 μL of 1× PBS formulations via lateral tail vein injections. PET whole-body acquisitions were recorded for mice at 4-48 h after injection while anesthetized with 1.5%–2.0% isoflurane in oxygen. The images were analyzed using ASIPro VM software (Concorde Microsystems).

Biodistribution Studies. Biodistribution studies were performed to measure the uptake of the radioconjugate in tumor and other relevant organs and tissues. After each time point, mice were euthanized by asphyxiation with CO_2. Blood was collected immediately via cardiac puncture while the tumor along with chosen organs was harvested. The wet weights of each tissue were calculated and the radioactivity bound to each organ was counted using standard γ-counters. The percentage of tracer uptake expressed as percentage injected dose per gram (% ID/g) was calculated as the activity bound to the tissue per organ weight per actual injected dose decay-corrected to the time of counting.

Autoradiography and Histology. Following PET imaging and biodistribution studies, a subset of tumors were embedded in optimal-cutting-temperature mounting medium and frozen on dry ice. Series of 10 μm frozen sections were then sliced at multiple tumor levels. To determine radiotracer distribution, digital autoradiography was performed by placing tissue sections in a

film cassette against a phosphor imaging plate (Fujifilm BAS-MS2325; Fuji Photo Film) for an appropriate exposure period at -20 °C (10 minutes for ^{18}F-FDG, and 96 hours for ^{89}Zr-Tf). Phosphor imaging plates were read at a pixel resolution of 25 μm with a Typhoon 7000 IP plate reader (GE Healthcare). After autoradiographic exposure, the same frozen sections were then used for immunohistochemical (IHC) staining and microscopy. Immunohistochemical staining of TfR and c-MYC were carried out using antibodies, along with TfR blocking peptide as a control (anti-c-MYC [Y69] ab32072, 10 μg/mL; anti-TfR ab84036, 4 μg/mL dilution, human transferrin receptor peptide ab101219, 10× excess), on both paraffin embedded (tumors fixed in neutral-buffered formalin upon excision) and fresh frozen tissue (same tissue used for autoradiography). Sequential sections were stained with hematoxylin and eosin stain. Immunohistochemical and autoradiographic images were registered using Panaroma Viewer and Fiji, respectively.

Statistical Considerations. Tumor uptake was determined from both biodistribution studies as previously described, or from the regions of interest (ROIs) drawn from acquired PET images using ASIPro image analysis software. Results of drawn ROIs were expressed as the average %ID/g. Automated image processing and analysis were used when possible for biodistribution and imaging experiments to eliminate human bias. All data was analyzed by the unpaired, two-tailed Student's *t*-test and differences at the 95% confidence level ($P < 0.05$) was considered statistically significant. Positive and negative controls were included whenever possible.

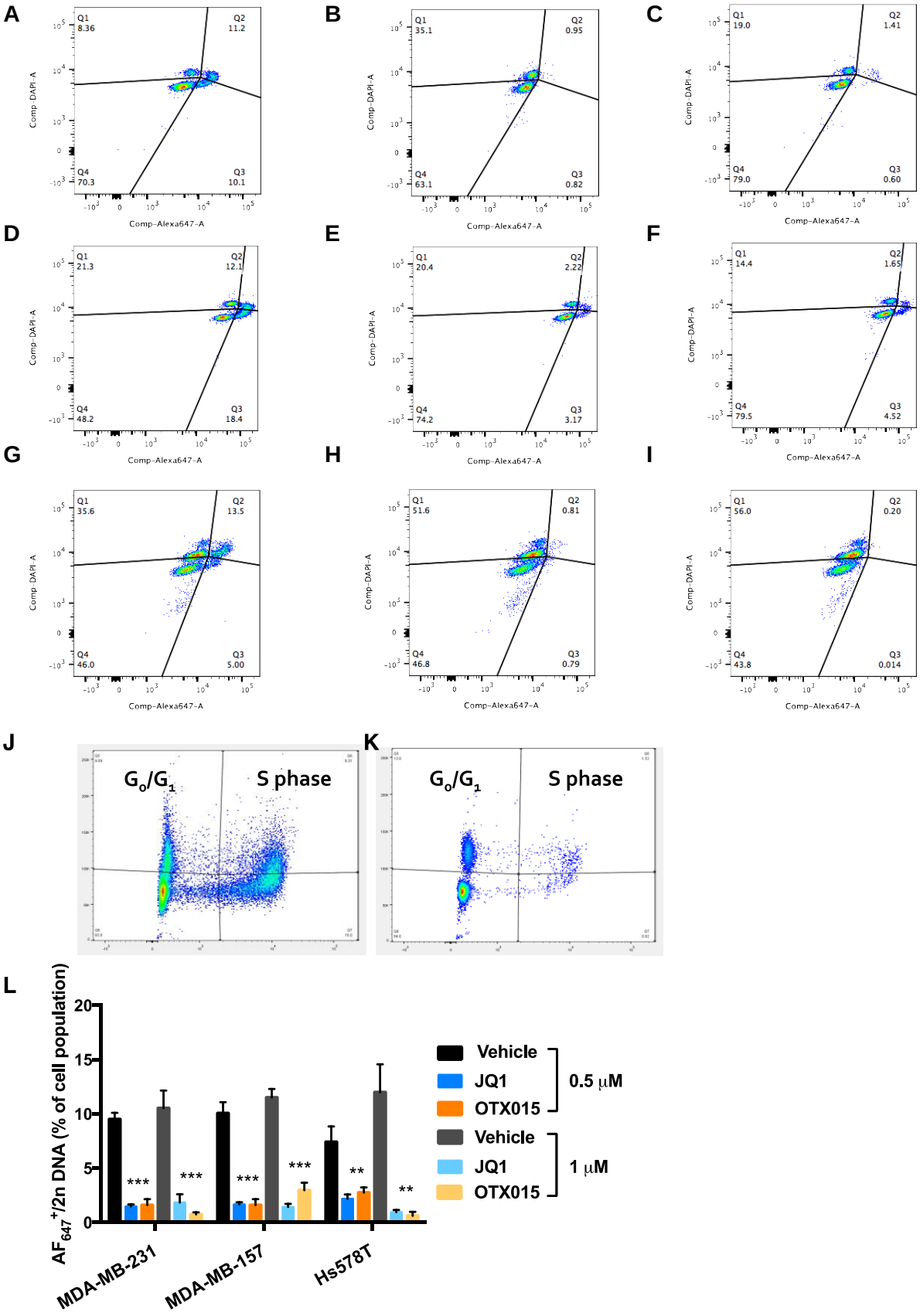
A
Q1 8.36
Q2 11.2
Q4 70.3
Q3 10.1
B
Q1 35.1
Q2 0.95
Q4 63.1
Q3 0.82
C
Q1 19.0
Q2 1.41
Q4 79.0
Q3 0.60
D
Q1 21.3
Q2 12.1
Q4 48.2
Q3 18.4
E
Q1 20.4
Q2 2.22
Q4 74.2
Q3 3.17
F
Q1 14.4
Q2 1.65
Q4 79.5
Q3 4.52
G
Q1 35.6
Q2 13.5
Q4 46.0
Q3 5.00
H
Q1 51.6
Q2 0.81
Q4 46.8
Q3 0.79
I
Q1 56.0
Q2 0.20
Q4 43.8
Q3 0.014
Comp-DAPI-A
Comp-Alexa647-A
J
K
G0/G1
S phase
L
AF647+/2n DNA (% of cell population)
20
15
10
5
0
***
***
***
***
**
**
MDA-MB-231
MDA-MB-157
Hs578T
Vehicle
JQ1
OTX015
0.5 μM
Vehicle
JQ1
OTX015
1 μM

Supplemental Figure 1. Representative dot plots of cell cycle analysis and % TNBC cells in S-phase as determined via flow cytometry. Cells were incorporated with EdU for 1 h prior to harvesting and staining protocol. (A-C) Vehicle, JQ1, and OTX015 treated MDA-MB-231 cells (1 μM), respectively. (D-F) Vehicle, JQ1, and OTX015 treated MDA-MB-157 cells (1 μM), respectively. (G-I) Vehicle, JQ1, and OTX015 treated Hs578T cells (1 μM), respectively. Representative zoomed in dot plot of MDA-MB-157 cells treated with vehicle (J) and JQ1 (K) at 500 nM. (L) Summary of % cell population in S-phase in vehicle vs. BRD4-treated TNBC cells. **P < 0.01, ***P < 0.001.

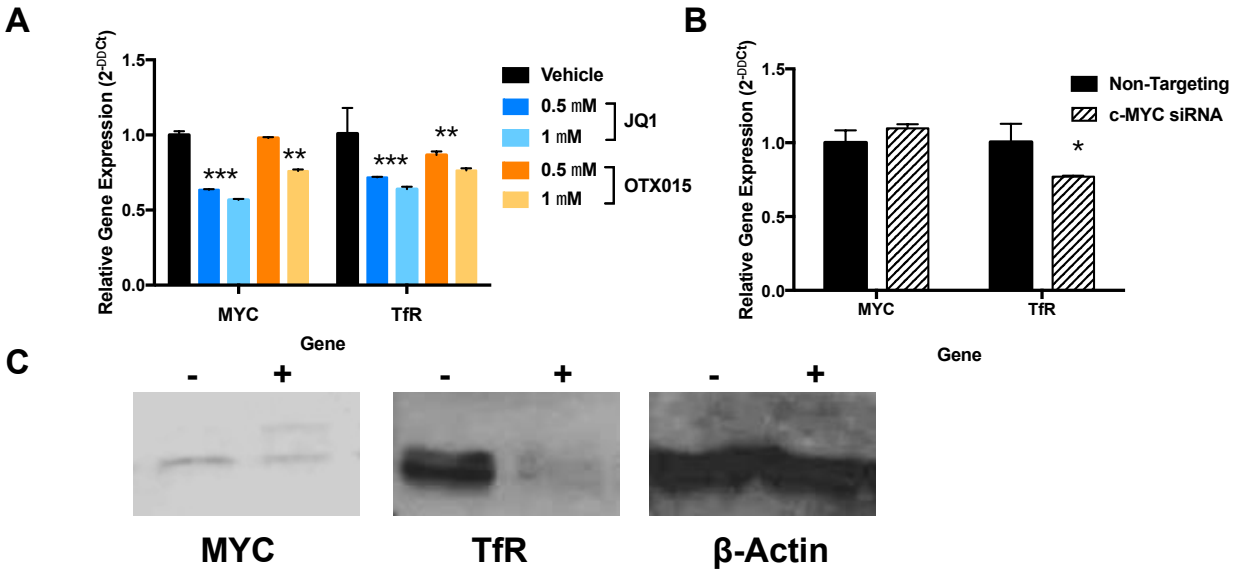

Supplemental Figure 2. Assessing the pharmacological and transcriptional effects of BRD4 inhibitors and c-MYC siRNA transfection on MYC and TfR gene expression in Hs578T TNBC cells. A dose-dependent decrease of MYC and TfR gene expression is decreased observed upon BRD4 inhibition (A) but only with TfR upon c-MYC siRNA knockdown (B). MYC and TfR protein levels are decreased upon c-MYC siRNA 48 h post-transfection (C). ***P < 0.001, **P < 0.01.

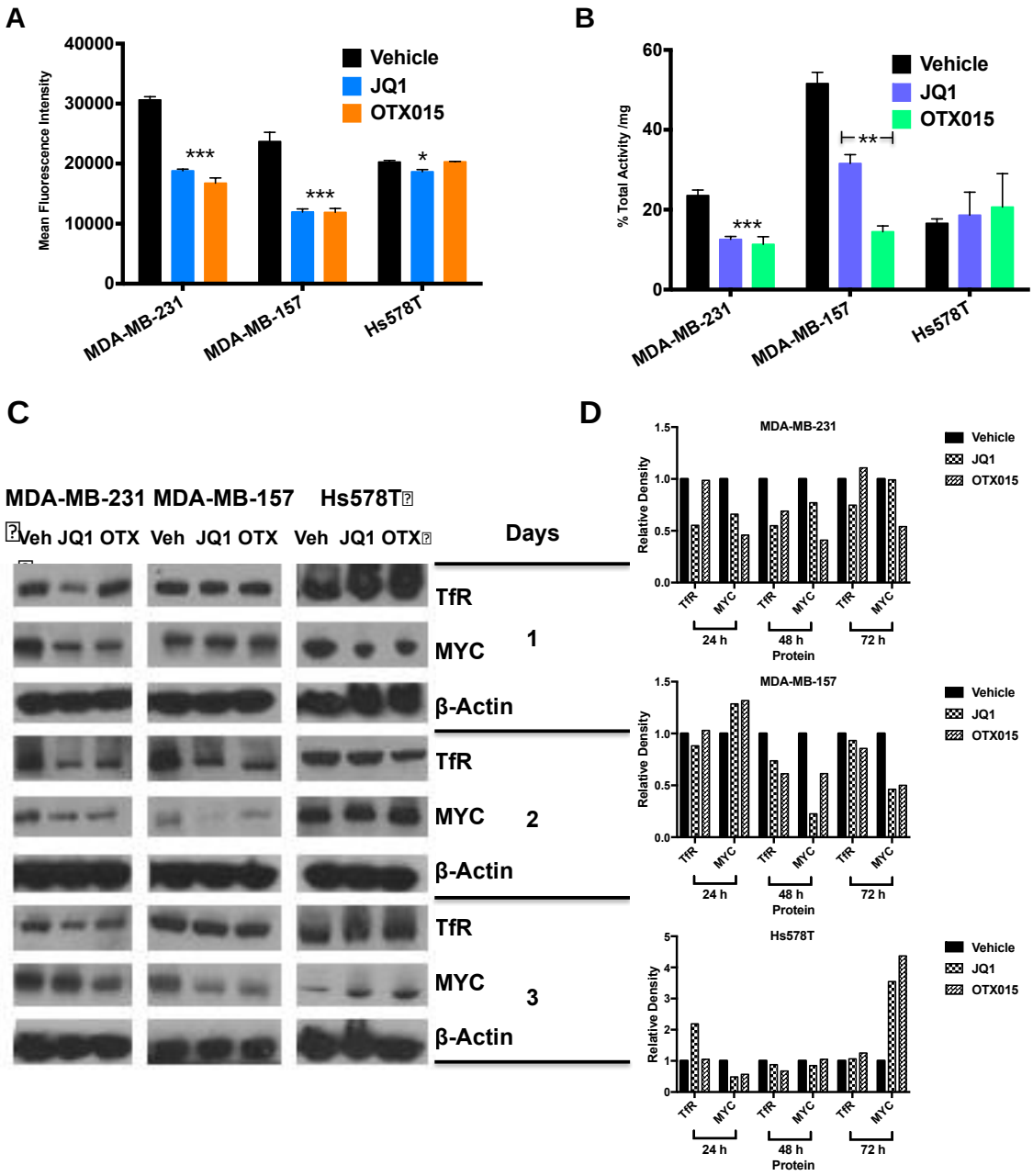

Supplemental Figure 3. Effects of BRD4 inhibitors on MYC and TfR protein levels in TNBC cells. (A) Surface TfR density decreases upon drug treatment over 48 h (500 nM) in MDA-MB-231 and MDA-MB-157 cells, while no response occurs in Hs578T cells at matching concentrations and time. (B) ^{131}I-transferrin internalization is significantly decreased in MDA-MB-231 and MDA-MB-157 cells upon drug treatment (500 nM, 48 h incubation). No significant response is noted for Hs578T cells. (C) MYC and TfR protein levels are decreased upon drug

treatment (500 nM, multiple time points) in MDA-MB-231 and MDA-MB-157 cells, and partially with Hs578T cells. (D) Densitometry analysis of western blot in part (C). ***P < 0.001, **P < 0.01, *P < 0.05.

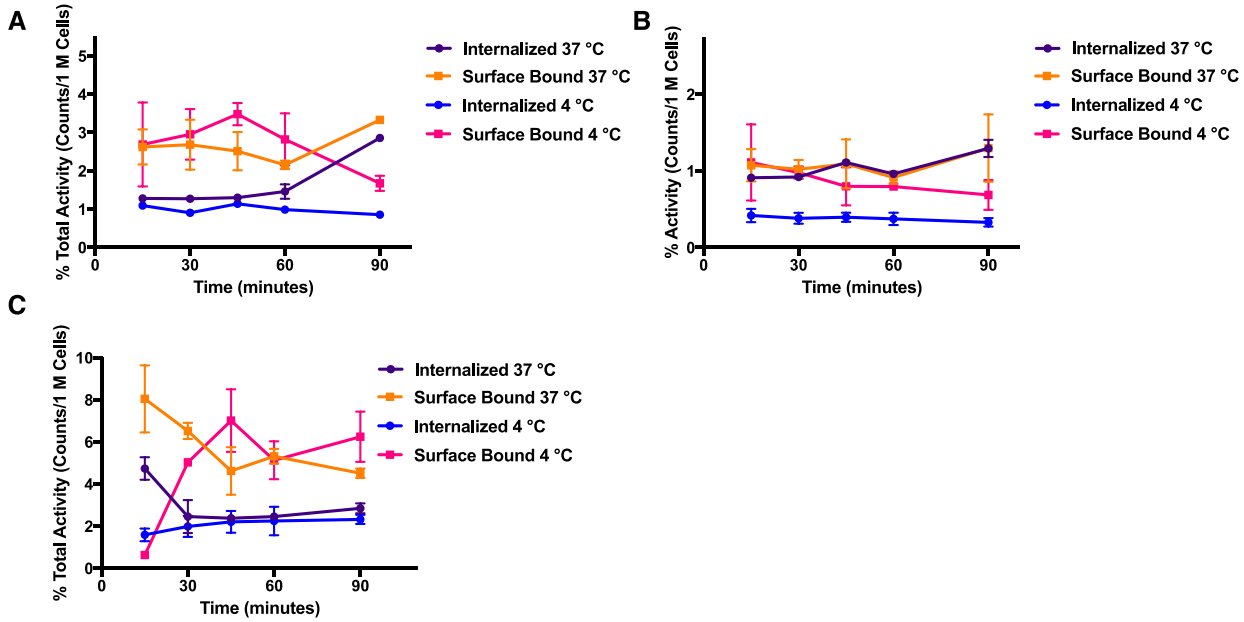

Supplemental Figure 4. Time-course internalization of ^{89}Zr-Tf in TNBC cell lines over the course of 90 minutes. Average internalized fraction was between 1-3 % for MDA-MB-231, (A) and MDA-MB-157 (B), and Hs578T cells (C). All data was normalized to 1 M cells.

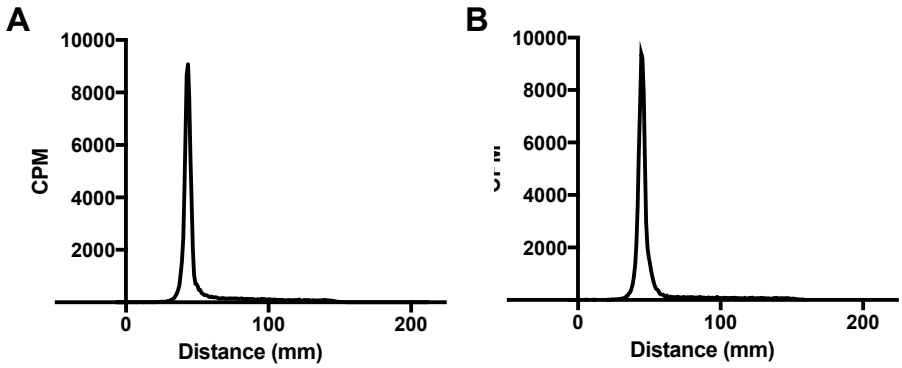

Supplemental Figure 5. Representative instant thin-layer chromatography of crude (A) and purified (B) ^{89}Zr-Tf labeling. Radiochemical purity was >99% for all experiments.

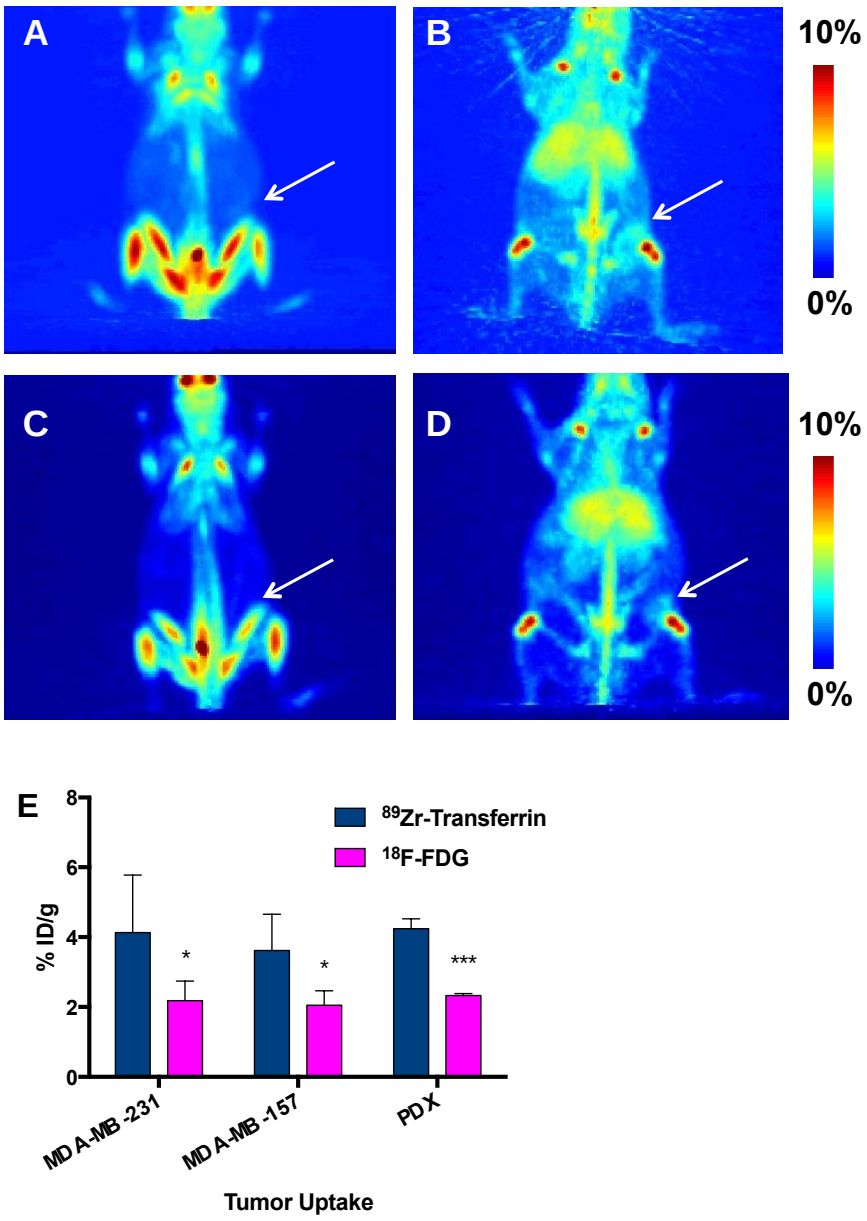

Supplemental Figure 6. Representative maximum intensity projections of ^{18}F-FDG uptake vs. ^{89}Zr-Tf in MDA-MB-231 tumor-bearing mice. Top images represent MIP of a larger tumor (~200 mm^3) of ^{18}F-FDG uptake (A) vs. ^{89}Zr-Tf uptake (B). The bottom images represent maximum intensity projections of ^{18}F-FDG (C) vs. ^{89}Zr-Tf uptake (D) in a smaller tumor (~50 mm^3). The same mice were used for ^{18}F-FDG and ^{89}Zr-Tf in each group, staggered by a 48 h period to ensure clearance of the ^{18}F-FDG, to confirm improved tumor targeting with ^{89}Zr-Tf.

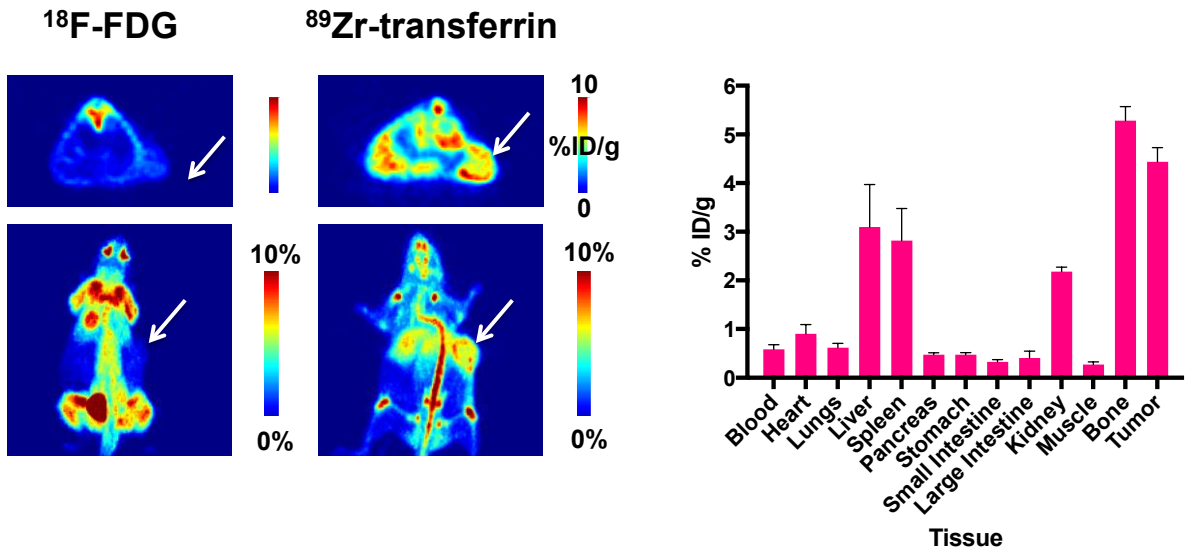

Supplemental Figure 7. Representative transverse (A and B) and maximum intensity projections (C and D) of ^{18}F-FDG uptake (left) vs. ^{89}Zr-Tf (right) in PDX tumor-bearing mice. (E) Full biodistribution of ^{89}Zr-Tf at 48 h in PDX mice. (F) Biodistribution comparison of ^{18}F-FDG vs. ^{89}Zr-Tf uptake in all TNBC tumors based on ROI analysis. ***P < 0.001, *P < 0.05.

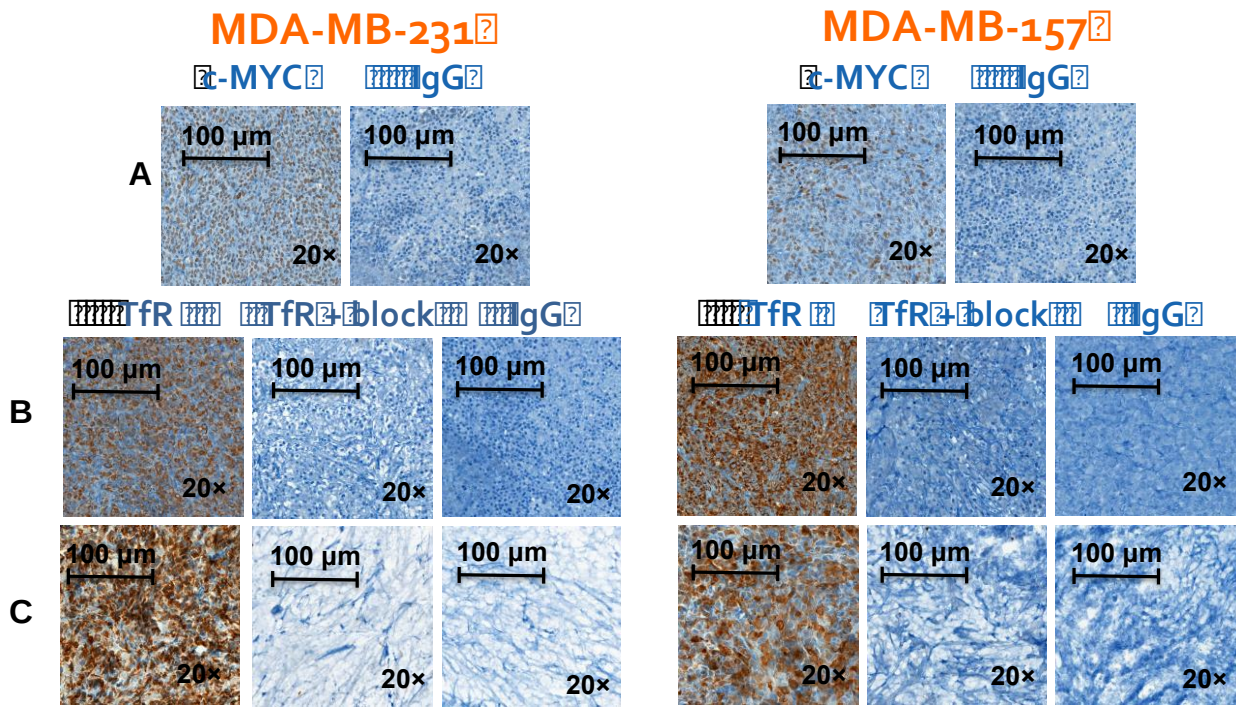

Supplemental Figure 8. Immunohistochemical analysis of TNBC tumors. (A) Abundance of c-MYC expression on paraffin embedded tissues compared to IgG control at matching concentrations. Abundance of TfR expression is represented in both paraffin-embedded (B) and fresh frozen tissue (C). A 10-fold excess of TfR blocking peptide was used as a control along with IgG at matching concentrations.

Supplemental Table 1. Full biodistribution of ^{18}F-FDG (1 h) and ^{89}Zr-Tf (48 h) in MDA-MB-231 and MDA-MB-157 xenografted mice. (*n* = 5/group).

	^{18}F-FDG						^{89}Zr-Tf					
Tissue	**MDA-MB-231**			**MDA-MB-157**			**MDA-MB-231**			**MDA-MB-157**		
Blood	0.8	±	1.0	0.3	±	0.1	3.2	±	1.6	1.8	±	0.6
Heart	9.9	±	4.1	19.2	±	6.5	2.2	±	0.6	1.8	±	0.6
Lungs	1.6	±	0.2	1.9	±	0.2	2.5	±	0.9	1.9	±	0.7
Liver	0.6	±	0.1	0.7	±	0.3	4.8	±	0.9	4.8	±	1.3
Spleen	1.5	±	0.4	1.5	±	0.1	5.1	±	1.0	4.9	±	2.7
Pancreas	0.9	±	0.2	1.0	±	0.2	4.1	±	0.5	4.1	±	1.1
Stomach	4.8	±	2.4	5.2	±	0.6	0.7	±	0.2	0.6	±	0.1
Small Intestine	7.1	±	1.6	6.9	±	2.4	1.8	±	0.7	2.4	±	0.7
Large Intestine	3.8	±	0.8	3.1	±	0.2	2.2	±	0.4	2.2	±	0.2
Kidney	1.0	±	0.3	0.8	±	0.1	4.5	±	2.8	2.1	±	0.2
Muscle	5.3	±	0.7	4.2	±	2.3	0.6	±	0.3	0.3	±	0.1
Bone	2.5	±	0.8	1.7	±	0.7	3.5	±	1.3	3.1	±	0.4
Tumor	2.3	±	0.0	2.2	±	0.5	3.6		0.9	4.1	±	1.3

Supplemental Table 2. Tumor: tissue ratios of ^{18}F-FDG (1 h) and ^{89}Zr-Tf (48 h) in MDA-MB-231 and MDA-MB-157 xenografted mice. Orange represents ratios that favor ^{89}Zr-Tf, purple represents ratios that favor ^{18}F-FDG, and blue represents no significant statistical difference between uptake for each radiotracer for both xenografts. (*n* = 5/group).

	^{18}F-FDG		^{89}Zr-TF	
Tumor to Tissue	**MDA-MB-231**	**MDA-MB-157**	**MDA-MB-231**	**MDA-MB-157**
Blood	2.9	6.6	1.8	2.3
Heart	0.2	0.1	2.0	2.3
Lungs	1.5	1.1	2.0	2.2
Liver	4.0	3.0	0.6	0.9
Spleen	1.5	1.5	0.6	0.8
Pancreas	2.5	2.2	3.4	1.0
Stomach	0.5	0.4	4.1	6.8
Small Intestine	0.3	0.3	3.8	1.7
Large Intestine	0.6	0.7	3.2	1.9
Kidney	2.3	2.6	0.8	2.0
Muscle	0.4	0.5	6.6	13.4
Bone	0.9	1.3	0.6	1.4

REFERENCES

1. Holland JP, Sheh Y, Lewis JS. Standardized methods for the production of high specific-activity zirconium-89. *Nucl Med Biol*. 2009;36(7):729-739.